

Electron diffusivities in MgB₂ from point contact spectroscopy

Y. Bugoslavsky, Y. Miyoshi, G. K. Perkins, A. D. Caplin, and L. F. Cohen
Blackett Laboratory, Imperial College London, SW7 2BZ, United Kingdom

A. V. Pogrebnyakov and X. X. Xi

Department of Physics and Materials Research Institute, Pennsylvania State University, University Park, Pennsylvania 16802, USA

(Received 23 March 2005; revised manuscript received 17 August 2005; published 9 December 2005)

We quantify the underlying physical mechanism behind the variation of the Andreev reflection with applied magnetic field in MgB₂ epitaxial film and find good agreement with the theory for a dirty two-band superconductor. The important microscopic property, the ratio of electron diffusivities in the σ and π bands can be measured directly by means of Andreev reflection. We analyze results obtained for different directions of the applied field and determine the anisotropy of the diffusivities demonstrating that the anisotropic upper critical field is determined solely by the anisotropic diffusivity in the σ band.

DOI: [10.1103/PhysRevB.72.224506](https://doi.org/10.1103/PhysRevB.72.224506)

PACS number(s): 74.70.Ad, 74.25.Ha, 74.50.+r

Magnesium diboride, MgB₂ is as yet a unique superconductor that has two distinct order parameters. They are derived from two groups of disconnected sheets of the Fermi surface (FS). Quasi-two-dimensional σ bands give rise to the larger superconducting gap, $\Delta_{\sigma} \sim 7$ meV, whereas the smaller gap, Δ_{π} opens up on the three-dimensional sheets of the FS that correspond to the π bands.^{1,2} First principle calculations of the electronic structure were successful in explaining the key normal-state properties of MgB₂. The theoretical description of superconducting properties in the presence of two bands has been developed on the basis of the Usadel equations, which are applicable to dirty-limit superconductors. Using this approach, the temperature dependence of the upper critical field H_{c2} ,³ the variation of the order parameters at the vortex core,⁴ the anisotropy of H_{c2} and the London penetration depth^{3,5} have all been calculated. The theoretical results are generally in good agreement with the available experiments, and provide guidance to engineering the material with desired properties. The elastic scattering rates in the two types of bands can be very different, as they are controlled by different kinds of atomic defects.⁶ Varying the ratio of electron diffusivities in the two bands (D_{σ}/D_{π}) will change the resulting macroscopic superconducting properties, and therefore independent determination of this ratio has emerged as a key prerequisite to understand and control the properties of MgB₂. Due to the crystalline anisotropy, the diffusivities along the c axis ($D_{\sigma,\pi}^{(c)}$) can be different from the in-plane values ($D_{\sigma,\pi}^{(a,b)}$). It is in principle possible to obtain the scattering rates from the temperature dependence of the resistivity,^{7,8} but this method is subject to large uncertainty if the sample is not 100% dense,⁹ which is often the case with MgB₂. In this work we demonstrate that the diffusivity ratio can be directly evaluated from point-contact Andreev reflection (PCAR) spectroscopy in magnetic field.

Point contact^{10–12} and tunneling spectroscopies,^{13,14} have been used to study the properties of MgB₂ in applied magnetic field. In Ref. 11 the point-contact results were linked to the theoretical density-of-states calculations⁴ and the diffusivities ratio was evaluated, but without revealing the physics

behind the observations, most importantly the effect of vortices. The scanning tunneling spectroscopy (STS) images of vortices parallel to the c axis¹⁵ have been successfully explained by theory.⁴ Importantly, vortex imaging is demanding experimentally and probes mainly the properties of the π band. It is possible to use the STS method to probe the in-plane vortices in sufficiently thick single crystals,¹⁴ but certainly not in thin films. The effect of vortices on the point-contact measurements has not been considered.

In our previous work¹⁵ we have demonstrated that as the field is increased, the transition to the normal state occurs simultaneously in the two superconducting subsystems, i.e., the σ and π bands are characterized by a unique H_{c2} . Later we have studied the evolution of the PCAR spectra with magnetic field in niobium;¹⁶ we showed that the mechanism behind the field variation of the Andreev reflection in Type-II superconductor is the presence of normal vortex cores, which leads to effective broadening of the spectra and increasing the zero-energy density of states (DOS), N^0 (corresponding to progressive increase of normal-state-like core excitations with increasing density of vortices). Therefore the PCAR data can be treated as a quantitative probe of the magnitude of N^0 . The theory⁴ predicts that in MgB₂ the DOS in the σ and π bands have distinctly different field dependences, which is a very specific conclusion that can be tested directly by experiment.

Here we discuss our results in the light of this theoretical prediction. We have found that in field parallel to the c axis there is a good agreement with the theory, in that the π -band DOS, N_{π}^0 increases with field much faster than the σ -band DOS. From the experiment we can directly extract the dependence $N_{\pi}^0(H)$ and hence, on the basis of Ref. 4, the value of D_{σ}/D_{π} . In our sample, there is strong disparity between the diffusivities, with the π band being relatively cleaner than the σ band. In theory³ increasing scattering in the π band would lead to a strong enhancement of H_{c2} at low temperatures. Although this is not the case in our sample, we demonstrate that the in-field point contact spectroscopy gives an insight into a highly relevant microscopic property of the two-band superconductor.

The measurements were performed on an epitaxial (c -axis

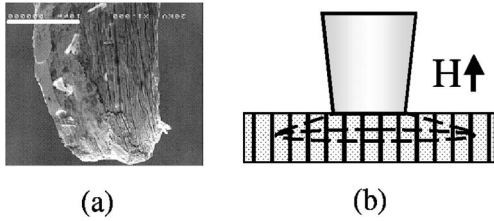


FIG. 1. (a) Scanning electron microscopy image of the gold tip after the point-contact measurements. The scale bar corresponds to 50 microns. The size of the deformed tip apex is indicative of the contact dimensions. (b) Schematic representation of the contact probing a large number of Abrikosov vortices (vertical lines) with the current injected into a large solid angle (dashed lines).

oriented) MgB_2 film grown by hybrid physical chemical vapor deposition (HPCVD).¹⁷ The critical temperature of the film was 39 K, an indication of negligible interband scattering. The value of $H_{c2\parallel c}$ was 6.5 T at 4.2 K, as obtained from resistivity measurements. The two-fold enhancement of H_{c2} compared to clean single crystals suggests that the film is closer to the dirty-limit superconductivity. The anisotropy of H_{c2} is a slowly varying function of temperature, increasing from 3 at $T=38.5$ K to 4 at 28 K.¹⁵ At lower temperatures the in-plane H_{c2} was too high to be measured with our 8-Tesla magnet. The point contact setup that we use is completely free of any magnetic parts, and mechanical stability of the contacts is independent of the magnetic field. The background resistance does not vary with field, which we take as a good indication of the contact geometry being invariant. Point contacts were made by pressing a sharpened gold tip to the surface of the film. The typical size of the contact footprint was 30 to 50 microns (see Fig. 1). However the sizes of the individual junctions at which the Andreev process occurs must be much smaller. Using the value of the contact resistance $R=10$ Ohm, residual resistivity of the film $\rho=10$ $\mu\text{Ohm cm}$ (Ref. 8) and the electron mean-free path $l\sim 100$ nm, it is possible to make an order-of-magnitude estimate of the junction size d . Using the formula for the resistance of a ballistic contact¹⁸ (Sharvin resistance), $R\sim\rho l/d^2$, we obtain $d\sim 30$ nm, which indicates that the junctions are in the ballistic regime, $d<l$. If the contact comprises multiple junctions, their individual sizes are less than 30 nm, so the ballistic regime can only be reinforced. Another evidence is that experimental spectra are well described by the ballistic, not diffusive regime of the BTK theory.¹⁹ For consistent interpretation of the effect of magnetic vortices on the Andreev reflection, we assume the contact comprises a number of small junctions randomly distributed across the contact area. The relevant length scale in a Type-II superconductor subjected to magnetic field is the distance between vortices, $a=\sqrt{2\Phi_0}/\sqrt{3H}$, where Φ_0 is the flux quantum. For example, in a field of 1 mT, the vortex separation is about 1 μm . Since our measurements were done at significantly higher fields, there was always a large number of vortices within the contact. We therefore presume that the current from the tip samples a random selection of microscopic junctions in an area large compared to the unit cell of the vortex lattice, and the results we obtain represent an effective average over the vortex lattice. We have demonstrated¹⁶ that

this interpretation provides a consistent agreement between experiment and the relevant theoretical calculations.²⁰ Importantly, we have confirmed experimentally that the results of the in-field measurements with Nb were independent of the mutual orientation of the field and the point-contact tip. This fact agrees with the premise that the current injection through a direct metal-superconductor junction is nondirectional. It is also plausible that surface roughness can contribute to the out-of-axis injection. These mechanisms explain why for any orientation of the vortex cores there is current that couples to the core excitations.

Similar to the case of Nb, here we write the conductance of the point contact in field as a sum of the “normal channel” (current injected into the cores) and the “SC channel” (current in between the vortices), extending this approach to combine it with the formulas used to describe the two-gap SC (e.g., Ref. 11). In zero field, the voltage-dependent normalized conductance of the point contact is then

$$\frac{G(V)}{G_N} = fg_\pi + (1-f)g_\sigma. \quad (1)$$

Here G_N is the normal-state junction conductance, and the normalized conductances g_π and g_σ are given by the usual expressions from the Blonder-Tinkham-Klapwijk (BTK) theory²¹ for the two values of the gap, Δ_π and Δ_σ , respectively. The shape of the functions g_π and g_σ is determined by the effective interface barrier Z ; we assume it is the same in the two bands. Typically the values of Z were found to be close to 0.5. The effects of finite temperature and interface scattering are taken into account by a convolution of the zero-temperature BTK functions with a Gaussian of width ω . In all the measurements reported here, the gold tip was perpendicular to the MgB_2 film, so that the “nominal” current direction was along the c axis. The fact that there is a contribution from the quasi-2D σ bands in this experimental geometry again confirms the nondirectional injection, which is characteristic of direct metal-superconductor contacts, and could be further facilitated by the fact that the surface of the MgB_2 film is not perfectly smooth due to columnar growth pattern.¹⁷ In Ref. 8 we have demonstrated that the contribution of the σ bands is correlated with the normal-state resistance ($R_N=1/G_N$) of the junction. Less transparent junctions (high R_N) have smaller amplitude of the σ peaks, and hence are more directional. The degree of directionality affects the value of the weighting f in Eq. (1). Therefore, if there were equal contributions to the DOS from the σ and π bands,²² we would still expect the geometrical factor to result in a higher measured weighting for the π band. The effect is difficult to quantify, and so we must rely on a best fit procedure for obtaining the value of f . We have found that typically $f=0.65-0.8$ in different contacts. We also make an assumption that in the applied field the deflection of current trajectories in the superconductor (e.g., due to Meissner screening) does not affect the nondirectionality of the injection.

In the presence of magnetic field, Eq. (1) needs to be modified to take into account the effect of normal cores. We do so by introducing two further variables, n_π and n_σ , to represent the field-dependent normal state contribution to the

differential conductance in each of the two bands. The resulting formula is

$$\frac{G(V)}{G_N} = f[n_\pi + (1 - n_\pi)g_\pi] + (1 - f)[n_\sigma + (1 - n_\sigma)g_\sigma]. \quad (2)$$

As n_π and n_σ represent the number of normal-state core excitations, these parameters can be identified with the zero-energy DOS N_π^0 and N_σ^0 , where the latter are understood as values averaged over the vortex lattice.

It is worth noting at this point that the properties of key significance for this work are n_π and n_σ ; importantly they enter Eq. (2) as simple scaling parameters. To a good approximation the conclusions on the behavior of n_π and n_σ are largely independent of the mathematical description of the functions g_π and g_σ . Therefore our results are not restricted to the particular regime of BTK theory but have a more general meaning, independent of the exact mathematical form used to model the zero-field Andreev spectra. To reflect this, and to eliminate problems with convergence of the multiparameter fitting procedure, we constrain some parameters in Eq. (2) to their zero-field values, as explained below.

The experiment in $H \parallel c$ corresponds to the situation considered theoretically in Ref. 4. The data and respective best fits to Eq. (2) are shown in Fig. 2(a). The fitting is performed in two steps. At zero field the fit to Eq. (1) is robust and we obtain the values of Z and f . Assuming that the interface properties (Z) and the injection geometry (f) remain the same unless the tip moves and the contact geometry changes, we treat these parameters as field-independent. In this case, adding two more variables in Eq. (2) (n_π and n_σ) for the in-field data does not compromise the robustness of the fit, so that the set of five parameters (Δ_π , Δ_σ , ω , n_π , and n_σ) can be extracted reliably. The field dependences of the order parameters, Δ_π , Δ_σ obtained from the present analysis are consistent with Ref. 15. In particular, we observe that Δ_π does not collapse at a field much smaller than the global H_{c2} . The effective broadening increases linearly with field. In principle, the form of $\Delta_\pi(H)$ and $\Delta_\sigma(H)$ can be used to evaluate the diffusivities ratio according to Ref. 4, but these functions are only weakly sensitive to the variation of diffusivities. In contrast, the effect on the behavior of n_π and n_σ is strong and hence it can be measured with greater accuracy.

The variation of the average DOS with field is presented in Fig. 3. The experimental data for the two field orientations (filled and open symbols, respectively) are plotted together with theoretical results for the case $D_\sigma^{(ab)}/D_\pi^{(ab)} = 0.5$.²³ The key experimental result here is a strong disparity between the field dependences of n_π and n_σ . At low fields both parameters exhibit closely linear increase with H . For $H \parallel ab$, the gradient of the $n_\sigma(H)$ dependence is close to $1/H_{c2}$, similar to both calculated and observed behavior for a conventional superconductor such as Nb.²⁰ In contrast, $n_\pi(H)$ has a gradient at low field that is four times as steep. These results are in qualitative agreement with the theory.⁴ Quantitatively, the values of the gradients are controlled by the ratio of electron diffusivities in the two bands, $D_\sigma^{(ab)}/D_\pi^{(ab)}$ (the in-plane diffusivities are relevant in this field orientation). It is the value of

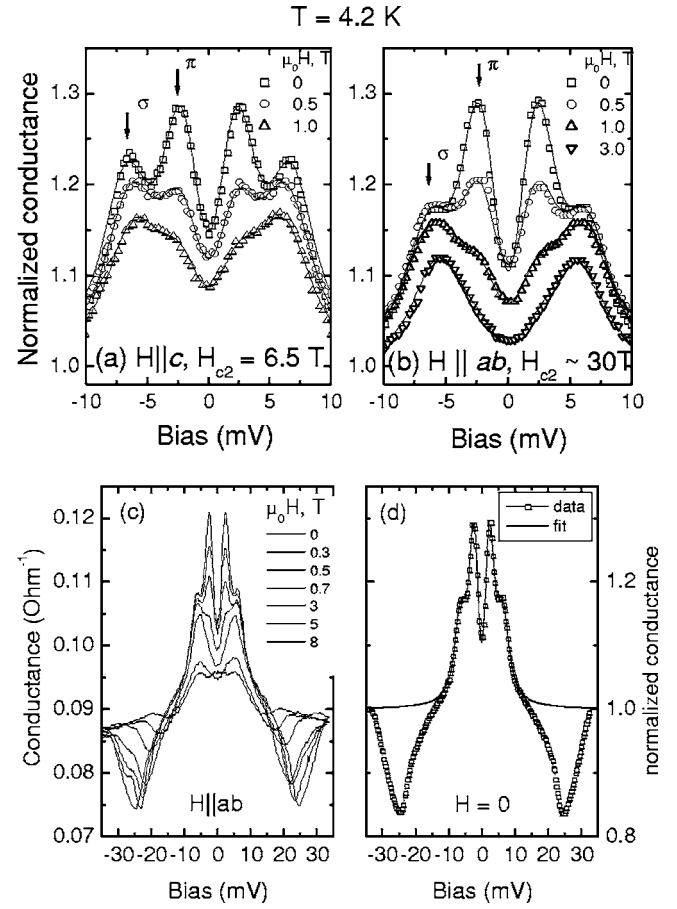


FIG. 2. Representative experimental data at 4.2 K and corresponding best fits to Eq. (2), (a) field parallel to the c axis; (b) field parallel to the ab plane. The data in field parallel to the ab plane are shown in (c) on a larger bias scale. The presence of a sloped background and extra high-bias features do not affect the quality of fit at the bias range of interest, as it is demonstrated in (d) for the zero-field, $H \parallel ab$ normalized spectrum.

dn_π/dH that is very sensitive to the variation of $D_\sigma^{(ab)}/D_\pi^{(ab)}$, with the gradient being steep for a relatively dirty σ band/clean π band ($D_\sigma^{(ab)}/D_\pi^{(ab)} < 1$). The conclusion is that the results of our experimental analysis in conjunction with the two-band dirty-limit theory can be used for accurate determination of the diffusivities ratio.

To take measurements in the field applied parallel to the ab plane, the sample and the tip were remounted and a new point contact was made. The central part of the normalized spectra for $H \parallel ab$ are shown in Fig. 2(b). The same data but on a larger bias scale is shown in Fig. 2(c). In this contact the normal-state conductance is weakly dependent on the bias, as it can be seen for the 8 Tesla curve at $|V| > 15$ mV. This effect is not related to superconductivity and we eliminate it from the analysis by way of normalizing all the data by the linearly varying background. Additionally, there are large field-dependent features at high bias (~ 25 mV), which are not accounted for by the BTK model. Indeed similar pronounced dips have been reported in point-contact experiments with various materials. Several possible mechanisms have been proposed to explain these features (proximity

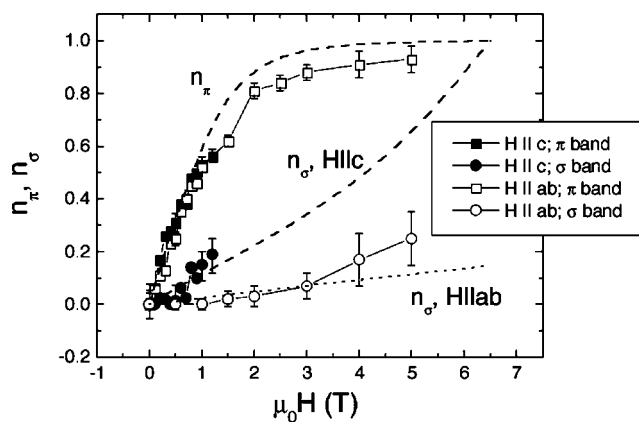


FIG. 3. Field variation of the normal state contribution to the DOS in the σ and π bands as a function of field, as inferred from the PCAR data using Eq. (2). Solid symbols, $H \parallel c$; open symbols, $H \parallel ab$; circles, σ band; squares, π band. The dashed lines are theoretical results (Ref. 22) for $H \parallel c$ and $D_{\sigma}^{(ab)}/D_{\pi}^{(ab)}=0.5$ and $H_{c2\parallel c}=6.5$ T. The dotted line shows the estimated theoretical behavior of the σ -band DOS in $H \parallel ab$.

effect,²⁴ Josephson effect,²⁵ influence of the critical current in the SC electrode²⁶), but no complete agreement between any of the models and the experiment has been attained. It has been pointed out²⁶ that the presence of the dips may signal that application of the BTK model can lead to overestimating the value of the SC gap. However this issue would only affect the interpretation of the zero-field curves but not the scaling analysis based on Eq. (2), from which our main conclusions stem. As it is demonstrated in Fig. 2(d) neither the normalization nor the presence of high-bias features compromises the quality of the fit to the central part of the spectra.

In field applied parallel to the ab plane of the sample, H_{c2} at $T=4.2$ K is beyond the reach of our magnet; we therefore extrapolate the slowly varying anisotropy factor from higher temperatures (as measured in Ref. 15) and evaluate

$H_{c2\parallel ab} \sim 30$ T. $n_{\pi}(H)$ does not scale with $H_{c2\parallel ab}$, but rather follows the same dependence for the two field orientations, hence the π -band diffusivity is effectively isotropic. On the contrary, the behavior of the σ -band normal state contribution does depend on the field direction. The theoretical consideration⁴ strictly applies to the case of the field applied parallel to the c axis. To have an indication of how the σ -band density of states could depend on the in-plane magnetic field, we scale the results for the c -axis up to the value of $H_{c2\parallel ab} \sim 30$ T (lower dotted line in Fig. 3) At fields below 3 T the experimental $n_{\sigma}(H)$ agrees with the thus obtained theoretical curve. At higher fields the accuracy of the fitting procedure deteriorates, as the spectra become smaller in amplitude and less resolved as the result of the field-induced broadening. Still the results clearly demonstrate that in both field orientations, the σ band is the dirtier one and so it always determines H_{c2} in our sample. Consequently,^{3,4} $D_{\sigma}^{(ab)}/D_{\sigma}^{(c)} \sim (H_{c2\parallel ab}/H_{c2\parallel c})^2 \sim 25$.

In conclusion, we have demonstrated that the field variation of the Andreev reflection spectra in an MgB_2 film can be consistently understood in terms of the dirty-limit theory of a double-band superconductor. In field applied parallel to the c axis, this method provides a direct means of measuring the ratio of band diffusivities. This independent evaluation of the diffusivities is particularly important for the analysis of the enhanced H_{c2} in MgB_2 films,²⁷ as the theory³ requires these parameters for calculating H_{c2} and its temperature dependence. The diffusivities are also key to understanding the anisotropy of H_{c2} and the behavior of the London penetration depth, and hence the microwave properties of MgB_2 .

The authors thank A. Gurevich, I. I. Mazin, and A. A. Golubov for useful discussions. The work at Penn State is supported in part by ONR under Grant No. N00014-00-1-0294 and by NSF under Grant No. DMR-0306746. This work was supported by the U.K. Engineering and Physical Sciences Research Council.

¹A. Y. Liu, I. I. Mazin, and J. Kortus, Phys. Rev. Lett. **87**, 087005 (2001).

²H. J. Choi *et al.*, Nature (London) **418**, 758 (2002).

³A. Gurevich, Phys. Rev. B **67**, 184515 (2003).

⁴A. E. Koshelev and A. A. Golubov, Phys. Rev. Lett. **90**, 177002 (2003).

⁵A. A. Golubov and A. E. Koshelev, Phys. Rev. B **68**, 104503 (2003).

⁶Steven C. Erwin and I. I. Mazin, Phys. Rev. B **68**, 132505 (2003).

⁷I. I. Mazin, O. K. Andersen, O. Jepsen, O. V. Dolgov, J. Kortus, A. A. Golubov, A. B. Kuz'menko, and D. van der Marel, Phys. Rev. Lett. **89**, 107002 (2002).

⁸Y. Bugoslavsky, Y. Miyoshi, G. K. Perkins, A. D. Caplin, L. F. Cohen, H. Y. Zhai, H. M. Christen, A. V. Pogrebnnyakov, X. X. Xi, and O. V. Dolgov, Supercond. Sci. Technol. **17**, S350 (2004).

⁹J. M. Rowell, S. Y. Xu, X. H. Zeng, A. V. Pogrebnnyakov, Qi Li,

X. X. Xi, J. M. Redwing, W. Tian, and Xiaoqing Pan, Appl. Phys. Lett. **83**, 102 (2003).

¹⁰P. Szabó, P. Samuely, J. Kacmarcik, T. Klein, J. Marcus, D. Fruchart, S. Miraglia, C. Marcenat, and A. G. M. Jansen, Phys. Rev. Lett. **87**, 137005 (2001).

¹¹R. S. Gonnelli, D. Daghero, A. Calzolari, G. A. Ummarino, V. Dellarocca, V. A. Stepanov, J. Jun, S. M. Kazakov, and J. Karpinski, Phys. Rev. B **69**, 100504(R) (2004).

¹²I. K. Yanson and Yu. G. Naidyuk, Low Temp. Phys. **30**, 261 (2004).

¹³M. R. Eskildsen, M. Kugler, S. Tanaka, J. Jun, S. M. Kazakov, J. Karpinski, and O. Fischer, Phys. Rev. Lett. **89**, 187003 (2002).

¹⁴M. R. Eskildsen, N. Jenkins, G. Levy, M. Kugler, O. Fischer, J. Jun, S. M. Kazakov, and J. Karpinski, Phys. Rev. B **68**, 100508(R) (2003).

¹⁵Y. Bugoslavsky, Y. Miyoshi, G. K. Perkins, A. D. Caplin, L. F. Cohen, A. V. Pogrebnnyakov, and X. X. Xi, Phys. Rev. B **69**,

- 132508 (2004).
- ¹⁶Y. Miyoshi, Y. Bugoslavsky, and L. F. Cohen, *Phys. Rev. B* **72**, 012502 (2005).
- ¹⁷X. H. Zeng, A. V. Pogrebnyakov, A. Kotcharov, J. E. Jones, X. X. Xi, E. M. Lysczek, J. M. Redwing, S. Y. Xu, J. Lettieri, D. G. Schlom, W. Tian, X. Q. Pan, and Z. K. Liu, *Nat. Mater.* **1**, 35 (2002).
- ¹⁸A. Wexler, *Proc. Phys. Soc. London* **89**, 927 (1966).
- ¹⁹I. I. Mazin, A. A. Golubov, and B. E. Nadgorny, *J. Appl. Phys.* **89**, 7576 (2001).
- ²⁰A. A. Golubov and M. Yu. Kupriyanov, *J. Low Temp. Phys.* **70**, 83 (1988).
- ²¹G. E. Blonder, M. Tinkham, and T. M. Klapwijk, *Phys. Rev. B* **25**, 4515 (1982).
- ²²A. Brinkman, A. A. Golubov, H. Rogalla, O. V. Dolgov, J. Kortus, Y. Kong, O. Jepsen, and O. K. Andersen, *Phys. Rev. B* **65**, 180517(R) (2002).
- ²³A. A. Golubov (private communication).
- ²⁴G. J. Strjkers, Y. Ji, F. Y. Yang, C. L. Chien, and J. M. Byers, *Phys. Rev. B* **63**, 104510 (2001).
- ²⁵L. Shan, H. J. Tao, H. Gao, Z. Z. Li, Z. A. Ren, G. C. Che, and H. H. Wen, *Phys. Rev. B* **68**, 144510 (2003).
- ²⁶G. Sheet, S. Mukhopadhyay, and P. Raychaudhuri, *Phys. Rev. B* **69**, 134507 (2004).
- ²⁷A. Gurevich, S. Patnaik, V. Braccini, K. H. Kim, C. Mielke, X. Song, L. D. Cooley, S. D. Bu, D. M. Kim, J. H. Choi, L. J. Belenky, J. Giencke, M. K. Lee, W. Tian, X. Q. Pan, A. Siri, E. E. Hellstrom, C. B. Eom, and D. C. Larbalestier, *Supercond. Sci. Technol.* **17**, 278, Suppl. S (2004).